Analytical and Bioanalytical Chemistry (2022) 414:1641–1649
https://doi.org/10.1007/s00216-021-03788-5

RESEARCH PAPER

A photonic crystal fiber–based fluorescence sensor for simultaneous and sensitive detection of lactic acid enantiomers

Zhongmei Chi[1,2] · Minmin Li[1] · Jia Xu[1] · Li Yang[1]

Received: 28 September 2021 / Revised: 7 November 2021 / Accepted: 10 November 2021 / Published online: 13 January 2022

Abstract

A photonic crystal fiber (PCF)–based fluorescence sensor is developed for rapid and sensitive detection of lactic acid (LA) enantiomers in serum samples. The sensor is fabricated by chemical binding dual enzymes on the inner surface of the PCF with numerous pore structures and a large specific surface area, which is suitable to be utilized as an enzymatic reaction carrier. To achieve simultaneous detection of L-LA and D-LA, the PCF with an aldehyde-activated surface is cut into two separate pieces, one of which is coated with L-LDH/GPT enzymes and the other with D-LDH/GPT enzymes. By being connected and carefully aligned to each other by a suitable sleeve tube connector, the responses of both L-LA and D-LA sensors are determined by laser-induced flourescence (LIF) detection. With the aid of enzyme-linked catalytic reactions, the proposed PCF sensor can greatly improve the sensitivity and analysis speed for the detection of LA enantiomers. The PCF sensor exhibits a low limit of detection of 9.5 μM and 0.8 μM, and a wide linear range of 25–2000 μM and 2–400 μM for L-LA and D-LA, respectively. The sensor has been successfully applied to accurate determination of LA enantiomers in human serum with satisfactory reproducibility and stability. It is indicated that the present PCF sensors would be used as an attractive analytical platform for quantitative detection of trace-amount LA enantiomers in real biological samples, and thus would play a role in disease diagnosis and clinical monitoring in point-of-care testing.

Keywords Lactic acid enantiomers · Photonic crystal fiber · Fluorescence sensor · Enzyme-linked catalytic reaction

Introduction

Lactic acid (LA) is the final product of anaerobic glycolysis in human organizations [1–5]. Both the optically active enantiomers, i.e., L-LA and D-LA, exist in healthy human bodies [6–11]. While the normal level of D-LA is only ~ 1.0% of L-LA, the elevated D-LA level in the blood and urine, which may be caused by an overproduction of intestinal bacteria, or in cases of infection, ischemia, or traumatic shock, would ultimately result in metabolic acidosis and lead to severe neurological symptoms [12, 13]. On the other hand, a high L-LA level can also lead to the drop in blood pH value in the body, and even acidosis in severe cases [14, 15]. For coronavirus disease 2019 (COVID-19), LA levels in blood have been proposed as an important indicator for its stratification, therapeutic effect evaluation, and prognosis estimation [16]. For understanding the relative contribution to metabolic acidosis, it is of great clinical importance to establish a rapid, sensitive, and effective analytical method to discriminate and detect LA enantiomers in body fluids.

Traditional analytical methods for analysis of LA enantiomers include capillary electrophoresis (CE), gas chromatography (GC), and high-performance liquid chromatography (HPLC) with a chiral stationary phase or a chiral mobile phase [17–21]. These methods generally require complicated instruments and thus would be difficult to be used in point-of-care testing (POCT), which is of great importance for rapid determination of LA levels in blood with a remote manner. In recent years, biosensors with high sensitivity and good selectivity have developed rapidly and have shown promising applications in various fields of POCT [22–26]. Considering LA analysis, while biosensors using the immobilized enzyme electrochemical approach were reported for detection of L-LA in biological

✉ Li Yang
yangl330@nenu.edu.cn

1 Key Laboratory of Nanobiosensing and Nanobioanalysis at Universities of Jilin Province, Department of Chemistry, Northeast Normal University, 5268 Renmin Street, Changchun 130024, Jilin, China

2 College of Chemistry and Materials Engineering, Bohai University, Jinzhou 121013, Liaoning, China

fluids [27–32], no such biosensor has been developed for the assay of LA enantiomers.

Here, we propose a novel photonic crystal fiber (PCF) fluorescence sensor which is developed based on an enzyme-linked catalytic reaction for high-performance detection of LA enantiomers. Owing to its unique properties, PCF opens up new applications in nonlinear devices, fiber lasers, high-power transmission, and many other fields [33–38]. In addition to guiding light in a hollow core, PCF can be considered analogous to a bundle of capillary tubes with an inner diameter of several micrometers and has several essential advantages for assaying trace-amount samples [39–41]. The micro-and nano-structured PCF can greatly reduce sample volume and the three-dimensional structure with a large specific surface area enhances the sensor. In addition, the short diffusion distance of the micro-channel results in a high mass transfer efficiency and short signal response time. In recent years, PCF has emerged as a promising material for fabrication of sensors for the assay of different targets. For example, Chen et al. proposed a novel hollow-core PCF volatile trace explosive sensor based on the fluorescence quenching [42]; Wang et al. developed a hollow-core-PCF-based miniaturized sensor for the detection of aggregation-induced-emission molecules [43]; Yang et al. developed a sensitive PCF-based immunosensor for the detection of alpha fetoprotein [44].

In this study, dual enzymes are immobilized on the inner surface of the PCF by chemical bonding to fabricate the sensor for simultaneous detection of LA enantiomers. PCF serves not only as a carrier for immobilized dual enzymes but also as a sample container and an enzyme-catalyzed reactor. The proposed PCF fluorescence sensor is used for simultaneous detection of L-LA and D-LA enantiomers. To achieve this purpose, the PCF with an aldehyde-activated surface is cut into two separate pieces, one of which is coated with L-LDH/GPT enzymes and the other with D-LDH/GPT enzymes, forming sensor L-LA and sensor D-LA. Both sensors are connected and carefully aligned to each other by a suitable sleeve tube connector, and the responses are determined by laser-induced flourescence (LIF) detection. With the aid of enzyme-linked catalytic reactions, the detection sensitivity of the sensor is improved. The proposed PCF sensors are sensitive with good reproducibility and stability. The sensors are successfully applied to determine LA enantiomers in human serum samples, and the results are in good agreement with those determined by the clinical kit method. The proposed method is expected to play a role in POCT for disease diagnosis and clinical monitoring.

Experimental section

Reagents and materials

L-LA and D-LA were purchased from Sigma-Aldrich (St. Louis, USA). L-Lactate dehydrogenase (L-LDH), D-lactate dehydrogenase (D-LDH), β-nicotinamide adenine dinucleotide (NAD^+), glutamic-pyruvic transaminase (GPT), and L-glutamic acid (L-Glu) were obtained from Shanghai Yuanye Bio-Technology Co., Ltd. (Shanghai, China). Sodium alginate, disodium hydrogen phosphate (Na_2HPO_4), sodium dihydrogen phosphate (NaH_2PO_4), and Tris-HCl were obtained from Beijing Chemical Works (Beijing, China). Human serum samples were provided by The First Bethune Hospital of Jilin University. Ultrapure water was supplied by a Milli-Q Water System (Millipore, MA, USA). All other chemicals were of analytical reagent grade and solutions were filtered through 0.22-μm filters prior to use.

PCF (LMA-20, length 5 cm, core diameter 20 μm, the voids average channel 4–5 μm) was provided by NKT Photonics A/S (Denmark). The inner surface morphology of the PCF sensors was observed using a scanning electron microscope (SEM) (Philip XL-30 ESEM-FEG). A Fourier transform infrared spectrometer (FTIR) (Nicolet 6700, Thermo Scientific) and a UV-vis spectrophotometer (Agilent Cary 7000) were used to characterize the PCF sensors.

Fabrication of PCF sensors

The procedure for fabrication of the sensor is schematically shown in Fig. 1. A PCF was first washed with 0.1 M HCl for 30 min and 0.1 M NaOH for 1 h to clean and hydrophilize the inner surface of the PCF. After being washed with water and dried under N_2, the PCF was then modified with primary amines by flushing it with 1% (v/v) 3-ADMS solution in toluene for 1 h and incubated at room temperature for 1 h. After being washed with toluene and dried under N_2, the PCF was rinsed with 2.5% (w/v) glutaraldehyde (GA) solution for 1 h and incubated at room temperature for another 1 h. Since the amine groups can bind to one of the aldehyde groups in GA, an aldehyde-activated surface of the PCF is produced. After rinsing with ultrapure water, the L-LDH/GPT (or D-LDH/GPT) solution was filled into the PCF by vacuum and incubated at 4 °C overnight. The aldehyde groups can form a covalent bond through the aldehyde amine condensation reaction; thus, dual enzymes (LDH and GPT) are covalently immobilized onto the PCF surface. After being washed with Tris buffer (pH 9, 100 mM) to remove unbound enzyme molecules, the prepared PCF sensors were stored in 4 °C when not in use.

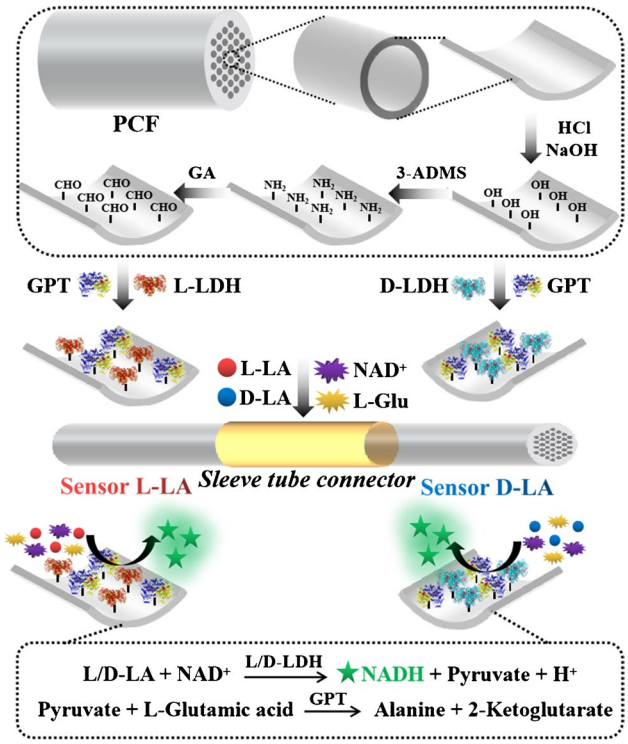

Fig. 1 Schematic diagram of the detection of LA enantiomers using the PCF fluorescence sensors

Sensing of LA enantiomers

The proposed PCF fluorescence sensors are used for simultaneous detection of L-LA and D-LA enantiomers. To achieve this purpose, a PCF with an aldehyde-activated surface was cut into two separate pieces. One was coated with L-LDH/GPT dual enzymes and the other was coated with D-LDH/GPT, forming the sensor L-LA and the sensor D-LA (see Fig. 1). For assaying the LA enantiomers, both PCF sensors were inserted into the sample mixture containing L/D-LA, NAD^+ and L-Glu, then they were connected and carefully aligned to each other by a suitable sleeve tube connector. After incubation for several minutes, selective enzyme-linked catalytic reactions of the enantiomers occurred to produce NADH in the corresponding sensor (that is, reactions of L-LA in sensor L-LA and those of D-LA in sensor D-LA). Finally, the fluorescence intensity of NADH from each sensor was measured using LIF detection.

An in-house-constructed LIF detection system was used to measure the fluorescence signal of the PCF sensors (see Electronic supplementary material Figure S1). The PCF sensors were inserted into a holder installed in a chamber made of black polytetrafluoroethylene (PTEF). A laser beam passed through a 375-nm band-pass filter (Beijing Bodian Optical Technology Co., Ltd., China) to produce a 375-nm monochromatic excitation light, which was focused on the PCF detection window through an optical convex lens (Beijing Zolix Instrument Co., Ltd., China). The fluorescence from the product NADH produced by the enzyme-linked catalytic reaction in the sensor was collected perpendicular to the excitation light. After being filtered by a 450-nm band-pass filter (Beijing Bodian Optical Technology Co., Ltd.) and passing a microscope objective, the fluorescence was measured by a photomultiplier tube (PMT) (CH-253, Beijing Hamamatsu Photon Technique INC) operated at 800 V. In our LIF system, the holder mounting the PCFs can be fine adjusted to allow the detection of the response of either sensor L-LA or sensor D-LA without changing the optical system of the LIF. A chromatography work station (Shanghai Vanshine Instrument Co., Ltd., China) was used to acquire the data.

Results and discussion

Characterization of the PCF sensor

Several spectroscopic techniques are utilized to characterize the immobilized-dual-enzyme PCF sensor. We first show in Fig. 2A–C the SEM images to characterize the morphology of the PCF sensor. PCF has 126 micro-channels with hexagonal symmetry which has good permeability and high mass transfer efficiency for the immobilization of enzymes (see Fig. 2A). Such a multi-channel structure can be viewed as a bunch of micro-capillaries, with a large specific surface area which can improve the response of the PCF sensor. The effect of dual-enzyme immobilization on the PCF inner surface can be observed in Fig. 2B, C. While the inner surface of a bare PCF is quite smooth (see Fig. 2B), the surface turns rough after LDH/GPT enzymes are immobilized (Fig. 2C).

Immobilization of enzymes on the PCF surface is further characterized by FTIR and UV-vis absorption spectra. Figure 2D shows the FTIR spectra of dual-enzyme-immobilized PCF (LDH/GPT-PCF), a bare PCF, and free enzymes. In the FTIR spectra of PCFs, strong absorption bands at 1100 cm^{-1} and 797 cm^{-1} can be attributed to Si–O–Si asymmetric stretching and Si–OH stretching vibrations, respectively. After enzyme immobilization, additional peaks at 1650 cm^{-1} and 1540 cm^{-1} appear in the spectrum of LDH/GPT-PCF, which can be assigned to C=O stretching vibration and N–H bending vibration of enzymes. Figure 2E presents the results of UV-vis absorption spectra. The characteristic absorption of proteins at 279 nm can be clearly seen in the spectrum of LDH/GPT-PCF, which is almost identical to the results of free enzymes. The results of both FTIR and UV-vis spectra strongly prove the successful immobilization of enzymes on the inner surface of the PCF.

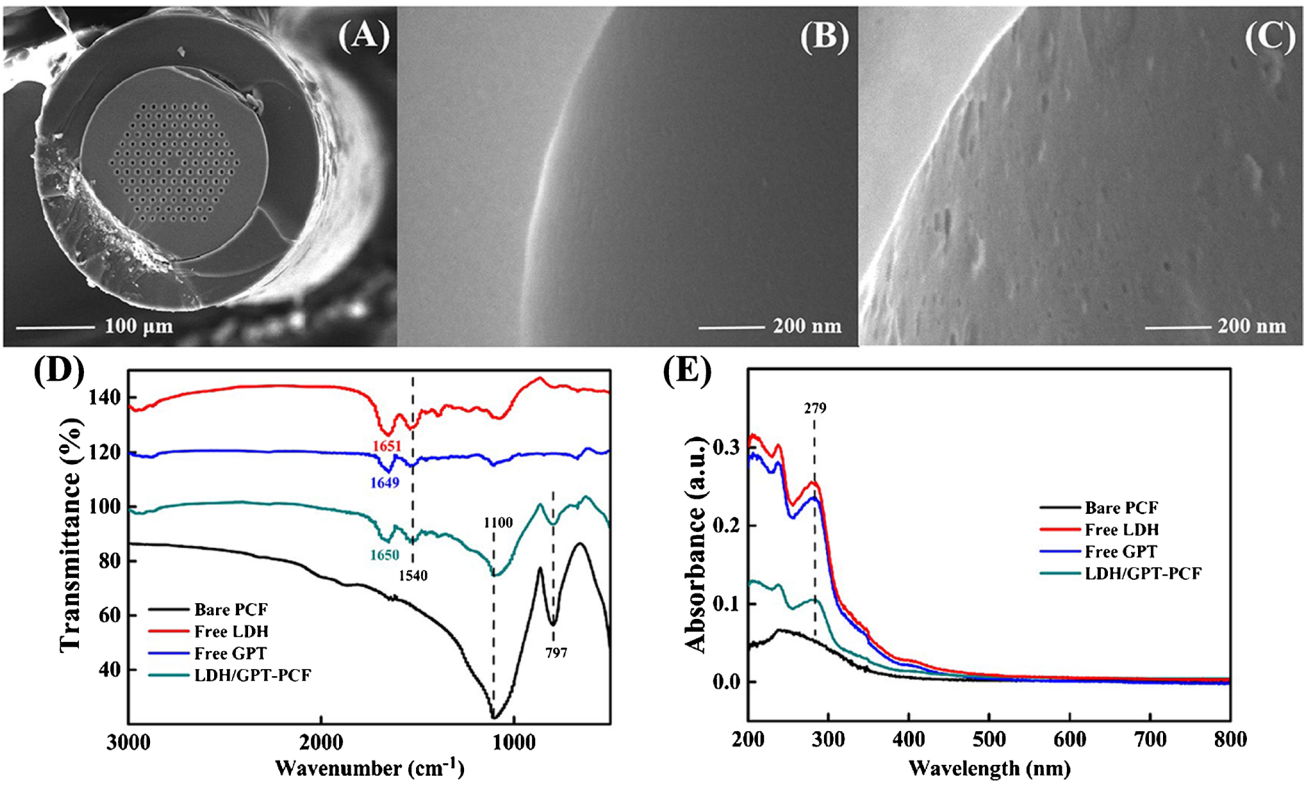

Fig. 2 SEM images of the cross section of a PCF (**A**) and the inner surface of a bare PCF (**B**) and a LDH/GPT-PCF (**C**); **D** FTIR and **E** UV-vis spectra of bare PCF, free LDH, free GPT, and LDH/GPT-PCF

Performance of the PCF sensor for the determination of LA enantiomers

The proposed PCF sensors can realize the sensitive detection of LA enantiomers based on LDH/GPT enzyme-linked synergistic catalytic reaction. The excitation wavelength of 375 nm and emission wavelength of 450 nm are used for fluorescence measurement. Figure S2 in the Electronic supplementary material presents the fluorescence intensity under different conditions, which verifies the feasibility of the enzyme-linked synergistic catalytic reaction for enhancement of the fluorescence signal. Several key factors, which are critical to the generation of NADH and thus would directly influence the detection sensitivity of the sensor, have been investigated and optimized. The results are presented in Figure S3 of the Supplementary material, including the concentration of LDH, the ratio of LDH/GPT, and the concentrations of NAD^+ and L-Glu. As shown in Figure S3A, the fluorescence intensity increases with the increase of L/D-LDH concentration in the range of 10–100 U/mL (for L-LDH) or 50–400 U/mL (for D-LDH). Considering both sensitivity and enzyme cost, the concentrations of L-LDH and D-LDH are chosen to be 50 U/mL and 200 U/mL, respectively. The effect of the concentration ratio of dual enzymes (LDH:GPT) on the fluorescence intensity is shown in Figure S3B, the results of which indicate that the optimal ratio of LDH/GPT is 1:1. For the concentration of coenzyme NAD^+, the maximal fluorescence intensity is observed at 4.5 mM in the range of 1–8 mM (see Figure S3C). Concerning the concentration of L-Glu, the fluorescent intensity tends to be saturated after the concentration is higher than 110 mM, indicating pyruvate produced by the enantiomeric reaction of LA is nearly consumed (see Figure S3D). We also investigate the effect of incubation time on the fluorescence intensity for the PCF sensor, as shown in Electronic supplementary material Figure S4. The results show that an incubation time of only 3 min or 5 min for L-LDH or D-LDH reaction is enough to achieve the best response of the sensor. To meet the requirement of simultaneous detection of LA enantiomers, the incubation time is selected as 5 min.

Under the optimal conditions for sensing, we evaluate the performance of the proposed PCF sensor. In Fig. 3A, B, we show the batch-to-batch reproducibility of sensor L-LA and sensor D-LA, respectively, and the results of the run-to-run reproducibility and day-to-day stability are presented in Fig. 3C, D, respectively. The sensor exhibits good batch-to-batch reproducibility with RSD ($n = 5$) of 0.86% and 1.12%, for sensing L-LA and D-LA, respectively. For run-to-run reproducibility, 10 continuous assays are performed by using one PCF sensor, and the fluorescence intensity

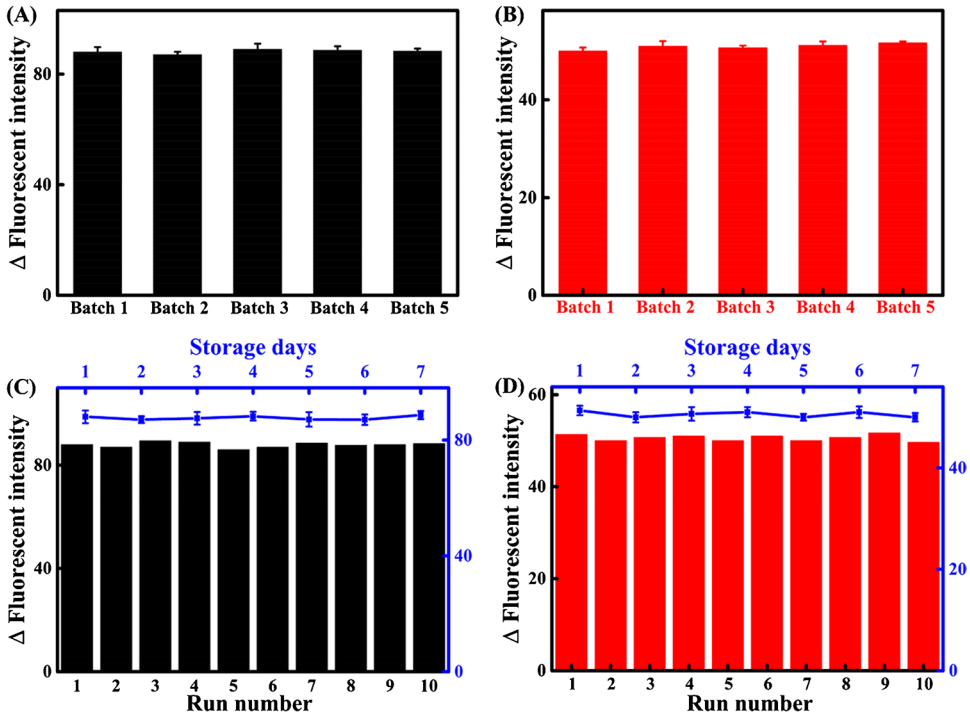

Fig. 3 Batch-to-batch reproducibility of the L-LA PCF sensor (**A**) and D-LA PCF sensor (**B**); run-to-run reproducibility and day-to-day stability of the L-LA PCF sensor (**C**) and D-LA PCF sensor (**D**). Other conditions are the same as in Figure S3. The excitation wavelength is 375 nm and the emission wavelength is 450 nm. The error bars represent the standard deviation of three replicated assays

remains almost unchanged (RSD (n = 10) of 1.19% and 1.31% for L-LA and D-LA). The day-to-day stability of the PCF sensors is evaluated over a period of 7 days. As indicated by the blue lines in Fig. 3C, D, no significant changes are observed in the response for either detection of L-LA or D-LA during 7 days, indicating excellent stability of the proposed PCF sensor.

The linear range and limit of detection (LOD) of the proposed PCF sensor for the detection of LA enantiomers are presented in Fig. 4A. The fluorescence intensity exhibits an excellent linear correlation to the concentration of L/D-LA. The linear detection ranges are 25–2000 μM ($Y = 0.3556X + 0.2737$, $R^2 = 0.9968$) and 2–400 μM ($Y = 2.2683X + 3.1596$, R^2=0.9983) for the detection of L-LA and D-LA, respectively, and the LOD are determined to be 9.5 μM and 0.8 μM. Figure 4B, C shows the selectivity of the proposed PCF sensor for the determination of L-LA and D-LA, respectively. Various chemicals, including urea, uric acid, ascorbic acid,

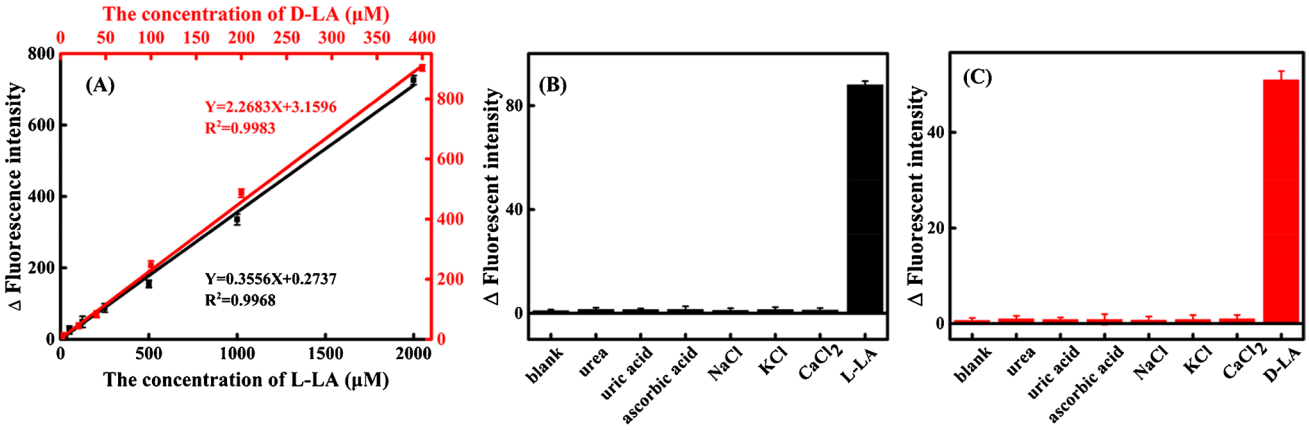

Fig. 4 **A** The linear relationship between the fluorescence intensity and L/D-LA concentration. **B** and **C** Selectivity of the PCF sensors for detection of L-LA and D-LA. The concentrations of L-LA and D-LA are 0.25 mM and 0.02 mM, and those of urea, uric acid, ascorbic acid, NaCl, KCl, and $CaCl_2$ are 10 mM. The conditions of the L-LA PCF fluorescence sensor: 50 U/mL L-LDH, L-LDH:GPT = 1:1, 4.5 mM NAD^+, 110 mM L-Glu, incubation time 5 min; D-LA PCF fluorescence sensor: 200 U/mL D-LDH, D-LDH:GPT = 1:1, 4.5 mM NAD^+, 110 mM L-Glu, incubation time 5 min. The excitation light power is 10 mW. The excitation wavelength is 375 nm and the emission wavelength is 450 nm. Δ fluorescence intensity is measured fluorescence intensity minus background fluorescence intensity. The error bars represent the standard deviation of three replicated assays

NaCl, KCl, and $CaCl_2$, are investigated as the interferents. It can be seen that even with a high concentration of 10 mM, neither of the interferents induces a significant fluorescence signal. The results indicate that the PCF sensor presents satisfactory selectivity for quantitative determination of the LA enantiomers.

Real sample analysis using the PCF sensors

To explore the applicability and feasibility of the proposed PCF fluorescence sensors for real sample assays, standard samples spiked with different concentrations of L/D-LA are analyzed. The results are presented in Table 1. The recoveries of L-LA and D-LA in human serum are in the range of 96.1–105.5% with RSD ($n = 3$) less than 9.3% and 96.9–103.4% with RSD ($n = 3$) less than 8.4%, respectively. This indicates that the proposed PCF sensor can achieve satisfactory accuracy and feasibility for the determination of LA enantiomers in human serum.

Table 1 L/D-LA recoveries in human serum using the PCF sensors

Sample (human serum)	Spiked	Measured	Recovery (%)	RSD (%) ($n = 3$)
L-LA/mM	0	1.26 ± 0.23	–	5.7
	0.1	1.34 ± 0.25	105.5	7.2
	0.2	1.47 ± 0.18	100.7	6.0
	0.5	1.69 ± 0.33	96.1	9.3
D-LA/μM	0	62.53 ± 0.45	–	3.5
	10	70.26 ± 0.68	96.9	6.6
	50	110.45 ± 0.54	98.2	5.7
	200	271.55 ± 0.76	103.4	8.4

Six clinical human serum samples are analyzed using the proposed PCF sensors, and the results are compared with the Megazyme lactate assay kit (K-DLATE, Beijing Microwise Co., Ltd., China). The relationship between our results and the Megazyme lactate assay kit results is shown in Fig. 5. It was found that the two methods have a good correlation, with the correlation coefficients of 0.9969 and 0.9973 for L-LA and D-LA, respectively. Our results show the capability of the proposed PCF sensors for the assay of LA enantiomers in human serum samples.

In Table 2, we compare the performance of the proposed PCF sensors for detection of LA enantiomers with those reported in the literature. The proposed method exhibits a low LOD with a short analysis time for assay of LA enantiomers. It is worth mentioning that our method can simultaneously determine LA enantiomers in several minutes without any complicated instruments, and thus would be of great value in POCT application for the detection of LA enantiomers in clinical biological samples.

Conclusion

In this study, we present a novel PCF sensor for sensitive detection of LA enantiomers. LDH/GPT dual enzymes are efficiently immobilized on the inner surface of the PCF via

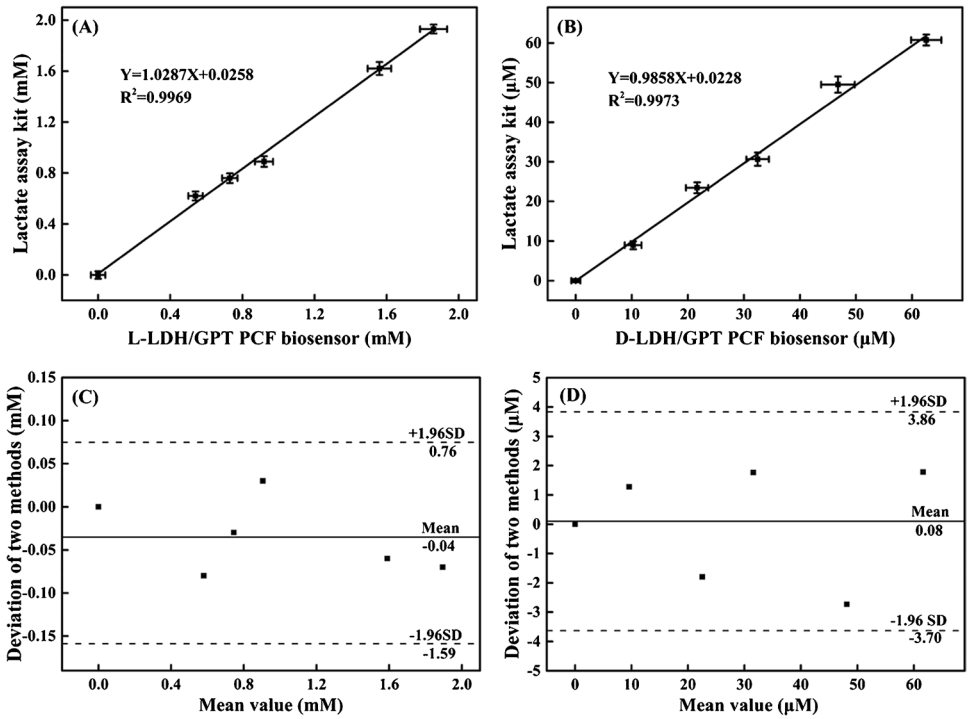

Fig. 5 Correlation and Bland-Altman analysis for the agreement between the PCF fluorescence sensors and Megazyme lactate assay kit for the determination of L-LA (**A**, **C**) and D-LA (**B**, **D**) in human serum samples. Data shows a 95% confidence interval of the mean for six human serum samples

Table 2 Comparison of the performances of different methods for the detection of LA enantiomers

Methods	Analytes	Linear range (μM)	LOD (μM)	Analysis time (min)	Refs
Electrochemical	L-LA	10–100	3	1	[45]
	D-LA	25–300	9		
HPLC	L-LA	500–4000	150	20	[7]
	D-LA	10–200	5.24		
GC-MS	L-LA	300–10,000	0.11	20	[6]
	D-LA	3–200	0.13		
CE	L-LA	25–5000	15	42	[46]
	D-LA	25–2500	20		
Enzymatic	L-LA	100–10,000	20	–	[47]
	D-LA	100–10,000	22		
PCF sensors	L-LA	25–2000	9.5	5	This work
	D-LA	2–400	0.8		

chemical bonding. Based on dual enzyme–linked catalytic reactions, the conversion of the LA enantiomers is enhanced to form fluorescent product NADH; thus, the response of the sensor is improved. Thanks to the multi-channel structure of PCF, the proposed PCF sensor is very sensitive for detection of L-LA and D-LA with LOD as low as 9.5 μM and 0.8 μM, respectively. In addition, the proposed PCF sensor shows several essential advantages, including rapid analysis with low sample consumption, high reproducibility and stability, and excellent selectively toward the LA enantiomers assay. As we have shown in the study, the PCF sensor is capable of being used to accurately determine LA enantiomers in real human serum samples. It is expected that the PCF-based biosensors would be promising in various disease diagnosis, clinical detection, and POCT applications.

Supplementary Information The online version contains supplementary material available at https://doi.org/10.1007/s00216-021-03788-5.

Acknowledgements This work is supported by the National Natural Science Foundation of China (Grant Nos. 21775017 and 22074014) and the Natural Science Foundation of Jilin Province, China (Grant No. 20200404153YY). The authors acknowledge the support from Jilin Provincial Department of Education.

Declarations

Ethics approval The human serum samples used in this study were approved by the Ethics Committee of The First Bethune Hospital of Jilin University in Changchun, China

Conflict of interest The authors declare no competing interests.

References

1. Choi YM, Lim H, Lee HN, Park YM, Park JS, Kim HJ. Selective nonenzymatic amperometric detection of lactic acid in human sweat utilizing a multi-walled carbon nanotube (MWCNT)-polypyrrole core-shell nanowire. Biosensors-Basel. 2020;10(9):111. https://doi.org/10.3390/bios10090111.
2. Ma LN, Huang XB, Muyayalo KP, Mor G, Liao AH. Lactic acid: a novel signaling molecule in early pregnancy? Front Immunol. 2020;11:279. https://doi.org/10.3389/fimmu.2020.00279.
3. Huang HC, Lee IJ, Huang C, Chang TM. Lactic acid bacteria and lactic acid for skin health and melanogenesis inhibition. Curr Pharm Biotechnol. 2020;21(7):566–77. https://doi.org/10.2174/1389201021666200109104701.
4. Li YS, Ju X, Gao XF, Zhao YY, Wu YF. Immobilization enzyme fluorescence capillary analysis for determination of lactic acid. Anal Chim Acta. 2008;610(2):249–56. https://doi.org/10.1016/j.aca.2008.01.049.
5. Zhang HY, Tan XX, Kang K, Wang W, Lian KQ, Kang WJ. Simultaneous determination of lactic acid and pyruvic acid in tissue and cell culture media by gas chromatography after in situ derivatization-ultrasound-assisted emulsification microextraction. Anal Bioanal Chem. 2019;411(3):787–95. https://doi.org/10.1007/s00216-018-1502-z.
6. Ding XM, Lin SH, Weng HB, Liang JY. Separation and determination of the enantiomers of lactic acid and 2-hydroxyglutaric acid by chiral derivatization combined with gas chromatography and mass spectrometry. J Sep Sci. 2018;41(12):2576–84. https://doi.org/10.1002/jssc.201701555.
7. Cevasco G, Piatek AM, Scapolla C, Thea S. A simple, sensitive and efficient assay for the determination of D- and L-lactic acid enantiomers in human plasma by high-performance liquid chromatography. J Chromatogr A. 2011;1218(6):787–92. https://doi.org/10.1016/j.chroma.2010.12.041.
8. Franco EJ, Hofstetter H, Hofstetter O. Determination of lactic acid enantiomers in human urine by high-performance immunoaffinity LC-MS. J Pharmaceut Biomed. 2009;49(4):1088–91. https://doi.org/10.1016/j.jpba.2009.01.033.
9. Sajewicz M, John E, Kronenbach D, Gontarska M, Kowalska T. TLC study of the separation of the enantiomers of lactic acid. Acta Chromatogr. 2008;20(3):367–82. https://doi.org/10.1556/AChrom.20.2008.3.5.
10. Shahangi F, Chermahini AN, Dabbagh HA, Teimouri A, Farrokhpour H. Enantiomeric separation of D- and L-lactic acid enantiomers by use of nanotubular cyclicpeptides: a DFT study. Comput Theor Chem. 2013;1020:163–9. https://doi.org/10.1016/j.comptc.2013.08.001.

11. Motonaka J, Katumoto Y, Ikeda S. Preparation and properties of enzyme sensors for l-lactic and d-lactic acids in optical isomers. Anal Chim Acta. 1998;368(1):91–5. https://doi.org/10.1016/S0003-2670(98)00188-3.
12. Pohanka M. D-Lactic acid as a metabolite: toxicology, diagnosis, and detection. BioMed Res Int. 2020;2020(2):1–9. https://doi.org/10.1155/2020/3419034.
13. Angell JW, Jones GL, Voigt K, Grove-White DH. Successful correction of D-lactic acid neurotoxicity (drunken lamb syndrome) by bolus administration of oral sodium bicarbonate. Vet Rec. 2013;173(8):193–3. https://doi.org/10.1136/vr.101536.
14. Zhou DD, Zeng K, Yang MH. Gold nanoparticle-loaded hollow Prussian Blue nanoparticles with peroxidase-like activity for colorimetric determination of L-lactic acid. Microchim Acta. 2019;186(2):7. https://doi.org/10.1007/s00604-018-3214-7.
15. Schuck A, Kim HE, Moreira JK, Lora PS, Kim YS. A graphene-based enzymatic biosensor using a common-gate field-effect transistor for L-lactic acid detection in blood plasma samples. Sensors. 2021;21(5):1852. https://doi.org/10.3390/s21051852.
16. Carlino MV, Valenti N, Cesaro F, Costanzo A, Cristiano G, Guarino M, et al. Predictors of Intensive Care Unit admission in patients with coronavirus disease 2019 (COVID-19). Monaldi Arch Chest Dis. 2020;90(3):430–6. https://doi.org/10.4081/monaldi.2020.1410.
17. Tsutsui H, Mochizuki T, Maeda T, Noge I, Kitagawa Y, Min JZ, et al. Simultaneous determination of DL-lactic acid and DL-3-hydroxybutyric acid enantiomers in saliva of diabetes mellitus patients by high-throughput LC-ESI-MS/MS. Anal Bioanal Chem. 2012;404(6-7):1925–34. https://doi.org/10.1007/s00216-012-6320-0.
18. Norton D, Crow B, Bishop M, Kovalcik K, George J, Bralley JA. High performance liquid chromatography-tandem mass spectrometry (HPLC/MS/MS) assay for chiral separation of lactic acid enantiomers in urine using a teicoplanin based stationary phase. J Chromatogr B. 2007;850(1-2):190–8. https://doi.org/10.1016/j.jchromb.2006.11.020.
19. Sonntag D, Fabian G, Scholtis S, Werner L. Gas chromatographic determination of lactic acid enantiomers by using a chiral stationary column. Dtsch Lebensm-Rundsch. 2004;100(9):348-351. https://www.researchgate.net/publication/289358897_Gas_chromatogr-aphic_determination_of_lactic_acid_enantiomers_by_using_a_chiral_stationary_column.
20. Todoroki K, Goto K, Nakano T, Ishii Y, Min JZ, Inoue K, et al. 4-(4,6-Dimethoxy-1,3,5-triazin-2-yl)-4-methylmorpholinium chloride as an enantioseparation enhancer for fluorescence chiral derivatization-liquid chromatographic analysis of DL-lactic acid. J Chromatogr A. 2014;1360:188–95. https://doi.org/10.1016/j.chroma.2014.07.077.
21. Henry H, Conus NM, Steenhout P, Beguin A, Boulat O. Sensitive determination of D-lactic acid and L-lactic acid in urine by high-performance liquid chromatography-tandem mass spectrometry. Biomed Chromatogr. 2012;26(4):425–8. https://doi.org/10.1002/bmc.1681.
22. Kim HE, Schuck A, Lee SH, Lee Y, Kang M, Kim YS. Sensitive electrochemical biosensor combined with isothermal amplification for point-of-care COVID-19 tests. Biosens Bioelectron. 2021;182:113168. https://doi.org/10.1016/j.bios.2021.113168.
23. Li ZD, Li F, Xing Y, Liu Z, You ML, Li YC, et al. Pen-on-paper strategy for point-of-care testing: rapid prototyping of fully written microfluidic biosensor. Biosens Bioelectron. 2017;98:478–85. https://doi.org/10.1016/j.bios.2017.06.061.
24. Castelli FA, Rosati G, Moguet C, Fuentes C, Marrugo-Ramírez J, Lefebvre T, et al. Metabolomics for personalized medicine: the input of analytical chemistry from biomarker discovery to point-of-care tests. Anal Bioanal Chem. 2021. https://doi.org/10.1007/s00216-021-03586-z.
25. Nie R, Huang J, Xu X, Yang L. A portable pencil-like immunosensor for point-of-care testing of inflammatory biomarkers. Anal Bioanal Chem. 2020;412(13):3231–9. https://doi.org/10.1007/s00216-020-02582-z.
26. Chen J, Meng HM, An Y, Liu J, Yang R, Qu L, et al. A fluorescent nanosphere-based immunochromatography test strip for ultrasensitive and point-of-care detection of tetanus antibody in human serum. Analy Bioanal Chem. 2020;412(5):1151–8. https://doi.org/10.1007/s00216-019-02343-7.
27. Maduraiveeran G, Chen AC. Design of an enzyme-mimicking NiO@Au nanocomposite for the sensitive electrochemical detection of lactic acid in human serum and urine. Electrochim Acta. 2021;368:7. https://doi.org/10.1016/j.electacta.2020.137612.
28. Arivazhagan M, Shankar A, Maduraiveeran G. Hollow sphere nickel sulfide nanostructures-based enzyme mimic electrochemical sensor platform for lactic acid in human urine. Microchim Acta. 2020;187(8):9. https://doi.org/10.1007/s00604-020-04431-3.
29. Calio A, Dardano P, Di Palma V, Bevilacqua MF, Di Matteo A, Iuele H, et al. Polymeric microneedles based enzymatic electrodes for electrochemical biosensing of glucose and lactic acid. Sensor Actuat B-Chem. 2016;236:343–9. https://doi.org/10.1016/j.snb.2016.05.156.
30. Ibupoto ZH, Shah S, Khun K, Willander M. Electrochemical L-lactic acid sensor based on immobilized ZnO nanorods with lactate oxidase. Sensors. 2012;12(3):2456–66. https://doi.org/10.3390/s120302456.
31. Gimenez-Gomez P, Gutierrez-Capitan M, Capdevila F, Puig-Pujol A, Fernandez-Sanchez C, Jimenez-Jorquera C. Monitoring of malolactic fermentation in wine using an electrochemical bienzymatic biosensor for L-lactate with long term stability. Analy Chim Acta. 2016;905:126–33. https://doi.org/10.1016/j.aca.2015.11.032.
32. Shimomura T, Sumiya T, Ono M, Ito T, Hanaoka T. Amperometric L-lactate biosensor based on screen-printed carbon electrode containing cobalt phthalocyanine, coated with lactate oxidase-mesoporous silica conjugate layer. Anal Chim Acta. 2012;714:114–20. https://doi.org/10.1016/j.aca.2011.11.053.
33. Portosi V, Laneve D, Falconi MC, Prudenzano F. Advances on photonic crystal fiber sensors and applications. Sensors. 2019;19(8):1892. https://doi.org/10.3390/s19081892.
34. Lv ZG, Teng H. Generation of wideband tunable femtosecond laser based on nonlinear propagation of power-scaled mode-locked femtosecond laser pulses in photonic crystal fiber. Chin Phys B. 2021;30(4):044209. https://doi.org/10.1088/1674-1056/abe231.
35. Zhang Y, Bu XQ. Narrow linewidth erbium-doped fiber laser incorporating with photonic crystal fiber based Fabry-Perot interferometer for temperature sensing applications. Optik. 2020;219:165005. https://doi.org/10.1016/j.ijleo.2020.165005.
36. Matsui T, Tsujikawa K, Okuda T, Hanzawa N, Sagae Y, Nakajima K, et al. Effective area enlarged photonic crystal fiber with quasi-uniform air-hole structure for high power transmission. IEICE Trans Commun. 2020;E103B(4):415–21. https://doi.org/10.1587/transcom.2019EBP3100.
37. Yan X, Shen RX, Cheng TL, Li SG. Research on filtering characteristics of asymmetric photonic crystal fiber based on gold coating. Opt Commun. 2021;488:126860. https://doi.org/10.1016/j.optcom.2021.126860.
38. Kazarian AA, Rodriguez ES, Deverell JA, McCord J, Muddiman DC, Paull B. Wall modified photonic crystal fibre capillaries as porous layer open tubular columns for in-capillary micro-extraction and capillary chromatography. Anal Chim Acta. 2016;905:1–7. https://doi.org/10.1016/j.aca.2015.10.005.
39. Kaur V, Singh S. A dual-channel surface plasmon resonance biosensor based on a photonic crystal fiber for multianalyte sensing.

J Comput Electron. 2019;18(1):319–28. https://doi.org/10.1007/s10825-019-01305-7.
40. Russell P. Photonic crystal fibers. Science. 2003;299(5605):358–62. https://doi.org/10.1109/JLT.2006.885258.
41. Yang X, Zhang AY, Wheeler DA, Bond TC, Gu C, Li Y. Direct molecule-specific glucose detection by Raman spectroscopy based on photonic crystal fiber. Anal Bioanal Chem. 2012;402(2):687–91. https://doi.org/10.1007/s00216-011-5575-1.
42. Yang JC, Shen R, Yan PX, Liu YH, Li XM, Zhang P, et al. Fluorescence sensor for volatile trace explosives based on a hollow core photonic crystal fiber. Sensor Actuat B-Chem. 2020;306:127585. https://doi.org/10.1016/j.snb.2019.127585.
43. Chen HF, Jiang QJ, Qiu YQ, Chen XC, Fan B, Wang Y, et al. Hollow-core-photonic-crystal-fiber-based miniaturized sensor for the detection of aggregation-induced-emission molecules. Anal Chem. 2019;91(1):780–4. https://doi.org/10.1021/acs.analchem.8b03219.
44. Liu XX, Song XD, Dong ZY, Meng XT, Chen YP, Yang L. Photonic crystal fiber-based immunosensor for high-performance detection of alpha fetoprotein. Biosens Bioelectron. 2017;91:431–5.
45. Matsui Y, Kitazumi Y, Shirai O, Kenji K. Simultaneous detection of lactate enantiomers based on diffusion-controlled bioeletrocatalysis. Anal Sci. 2018;34(10):1137–42. https://doi.org/10.2116/analsci.18P202.
46. Tan L, Wang Y, Liu XQ, Ju HX, Li JS. Simultaneous determination of L- and D-lactic acid in plasma by capillary electrophoresis. J Chromatogr B. 2005;814(2):393–8.
47. Girotti S, Muratori M, Fini F, Ferri EN, Carrea G, Koran M, et al. Luminescent enzymatic flow sensor for D- and L-lactate assay in beer. Eur Food Res Technol. 2000;210(3):216–9. https://doi.org/10.1007/PL00005515.